Supplementary information

Critical Assessment of Theoretical Modelling of Single-Atom Catalysts

Halil Bilgin, Alessandro Bonardi, Matteo Spotti, Giovanni Di Liberto, Gianfranco Pacchioni*

Department of Materials Science, University of Milano-Bicocca, Via Cozzi 55, 20125 Milano, Italy

Adsorption properties of 4N-Gr support and TM@4N-Gr

4N-Gr support (no TM present)

Table S1: Adsorption energy and Gibbs free energy of H* on all possible adsorption sites of 4N-Gr.

Adsorption site of H*	ΔE_{ads} /eV	ΔG_{ads} /eV	η /V
N	-1.87	-1.63	1.63
C5	1.31	1.55	1.55
C6	1.07	1.31	1.31
C7	1.11	1.35	1.35
C8	1.17	1.41	1.41
C10	1.24	1.48	1.48
C16	0.97	1.21	1.21
C18	0.70	0.94	0.94
C19	1.29	1.53	1.53

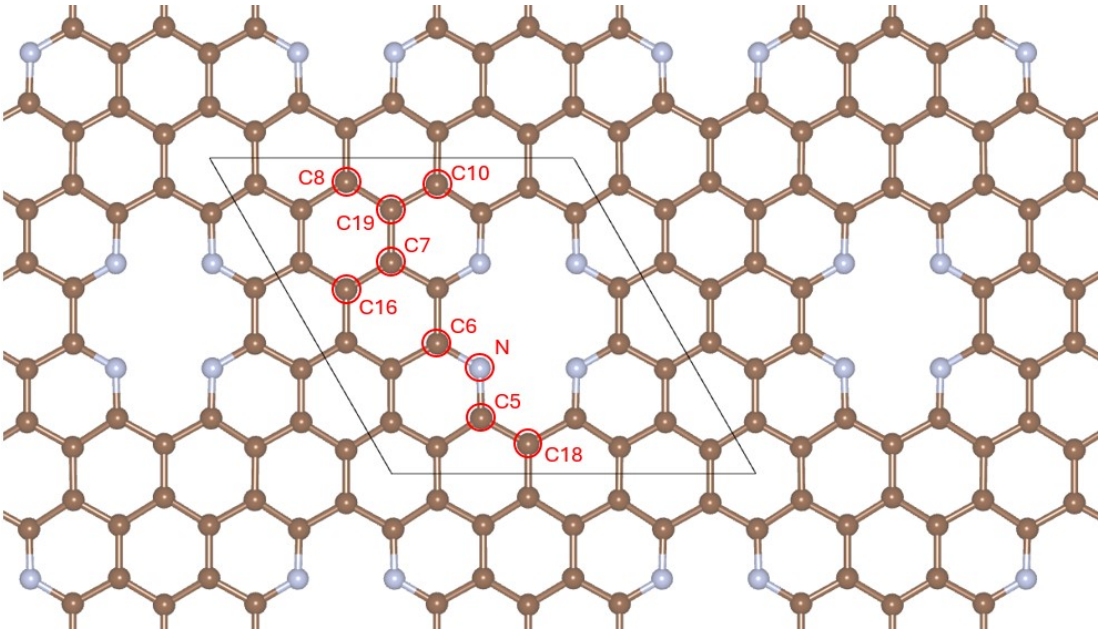

Figure S1: Possible adsorption sites of H* on 4N-Gr.

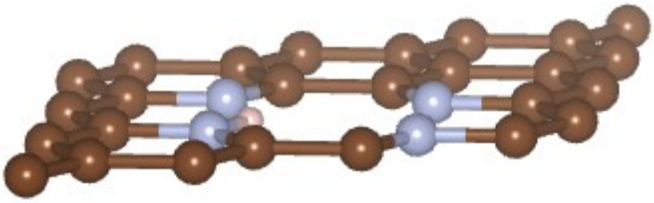

Figure S2: Adsorption configuration of H* on N-site of 4N-Gr.

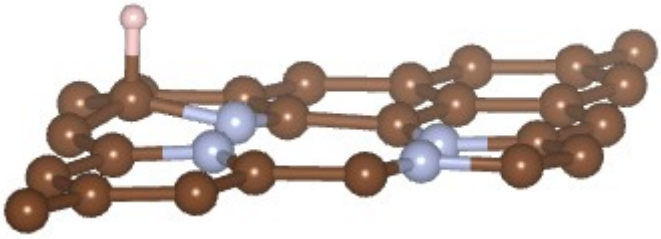

Figure S3: Adsorption configuration of H* on C5-site of 4N-Gr.

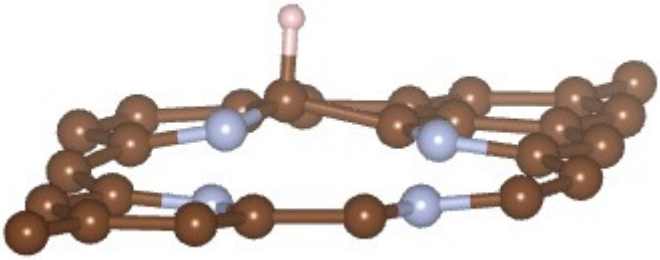

Figure S4: Adsorption configuration of H* on C6-site of 4N-Gr.

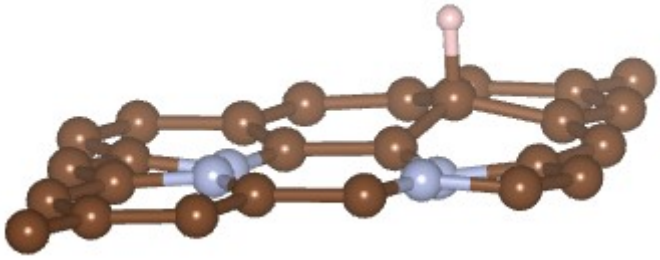

Figure S5: Adsorption configuration of H* on C7-site of 4N-Gr.

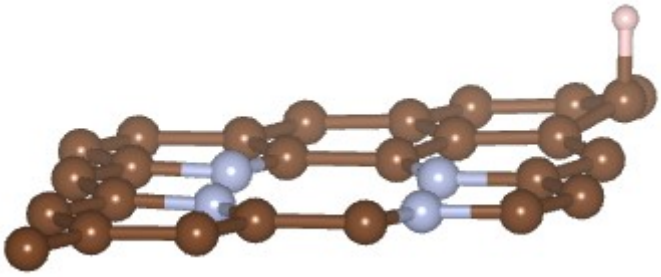

Figure S6: Adsorption configuration of H* on C8-site of 4N-Gr.

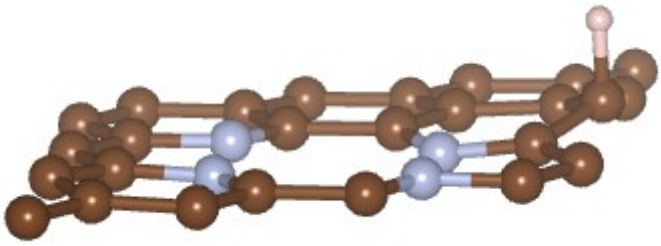

Figure S7: Adsorption configuration of H* on C10-site of 4N-Gr.

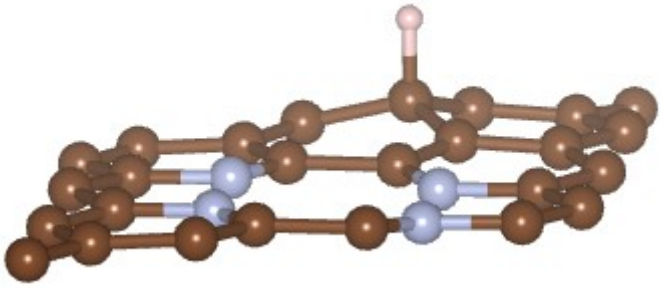

Figure S8: Adsorption configuration of H* on C16-site of 4N-Gr.

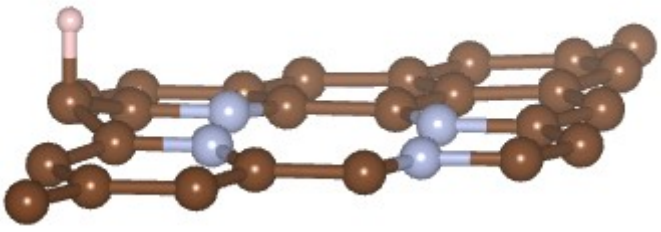

Figure S9: Adsorption configuration of H* on C18-site of 4N-Gr.

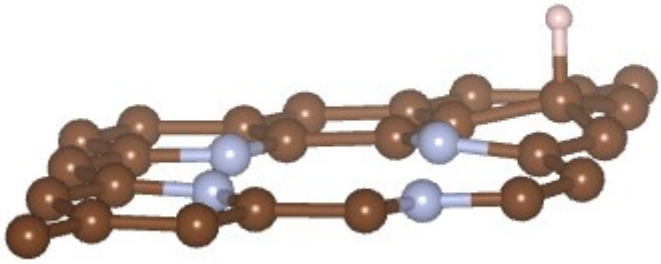

Figure S10: Adsorption configuration of H* on C19-site of 4N-Gr.

Ti@4N-Gr

Table S2: Binding energy and protrusion of Ti atom embedded in 4N-Gr matrix.

System	$\Delta E_{binding}$ /eV	Protusion /Å
Ti@4N-Gr	-8.28	0.00

Table S3: Adsorption energy and Gibbs free energy of H* on metal and near-metal adsorption sites of Ti@4N-Gr.

Adsorption site of H*	ΔE_{ads} /eV	ΔG_{ads} /eV	η /V
Ti	-1.09	-0.85	0.85
N	0.58	0.82	0.82
C	0.14	0.38	0.38
C1	0.12	0.36	0.36
C2	0.65	0.89	0.89

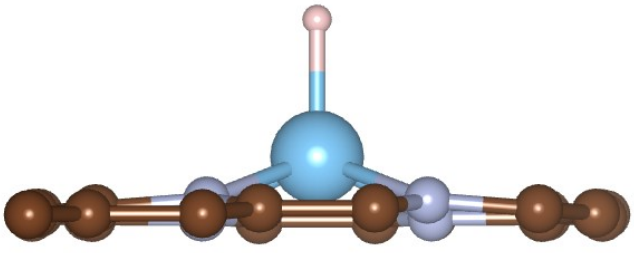

Figure S11: Adsorption configuration of H* on Ti-site of Ti@4N-Gr.

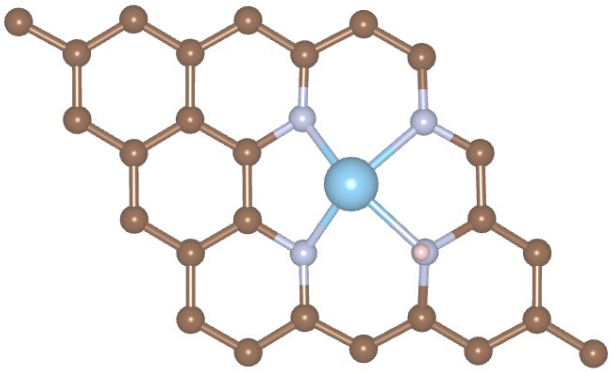

Figure S12: Adsorption configuration of H* on N-site of Ti@4N-Gr.

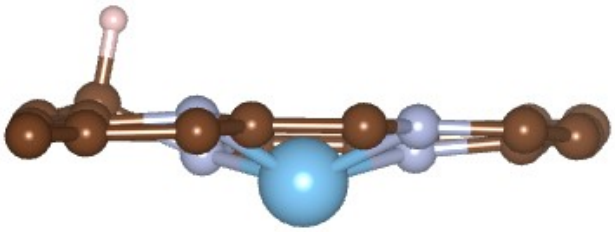

Figure S13: Adsorption configuration of H* on C-site of Ti@4N-Gr.

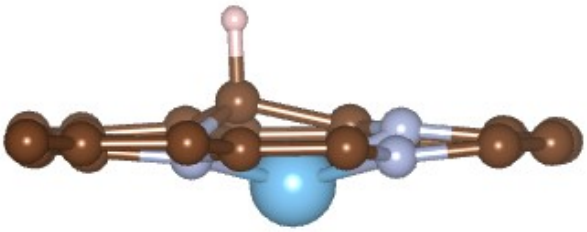

Figure S14: Adsorption configuration of H* on C1-site of Ti@4N-Gr.

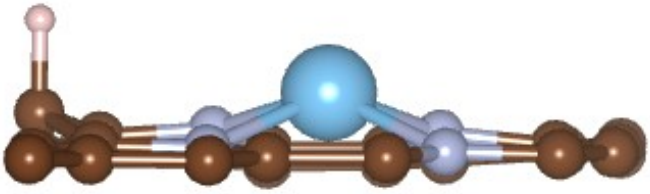

Figure S15: Adsorption configuration of H* on C2-site of Ti@4N-Gr.

Rh@4N-Gr

Table S4: Binding energy and protrusion of Ce atom embedded in 4N-Gr matrix.

System	$\Delta E_{binding}$ /eV	Protusion /Å
Rh@4N-Gr	-7.86	0.00

Table S5: Adsorption energy and Gibbs free energy of H* on metal and near-metal adsorption sites of Rh@4N-Gr.

Adsorption site of H*	ΔE_{ads} **/eV**	ΔG_{ads} **/eV**	η **/V**
Rh	-0.53	-0.29	0.29
N	\	\	\
C	1.07	1.31	1.31
C1	0.58	0.82	0.82
C2	0.50	0.74	0.74

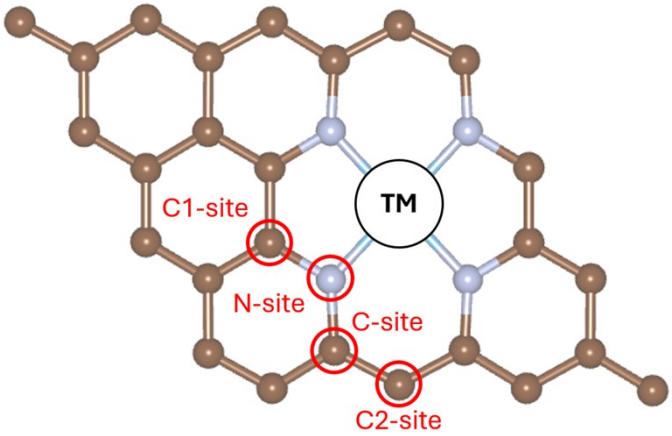

Figure S16: Possible adsorption near-metal sites of H* on TM@4N-Gr.

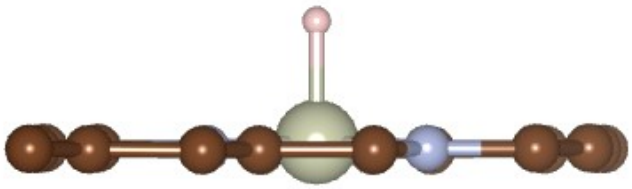

Figure S17: Adsorption configuration of H* on Rh@4N-Gr.

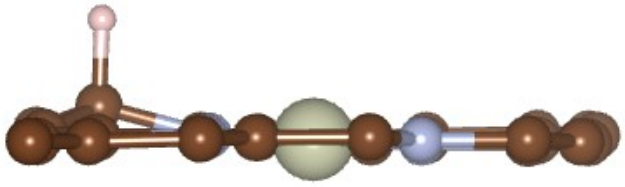

Figure S18: Adsorption configuration of H* on C-site Rh@4N-Gr.

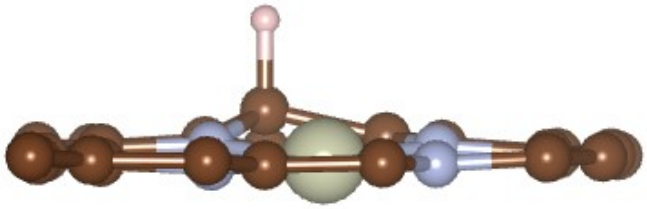

Figure S19: Adsorption configuration of H* on C1-site Rh@4N-Gr.

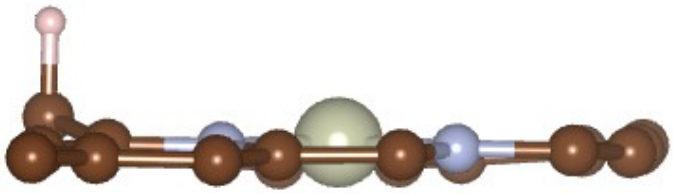

Figure S20: Adsorption configuration of H* on C2-site Rh@4N-Gr.

Ce@4N-Gr

Table S6: Binding energy and protrusion of Ce atom embedded in 4N-Gr matrix.

System	$\Delta E_{binding}$ /eV	Protrusion /Å
Ce@4N-Gr	-8.58	1.24

Table S7: Adsorption energy and Gibbs free energy of H* on Ce-site of Ce@4N-Gr.

Intermediate	ΔE_{ads} /eV	ΔG_{ads} /eV	η /V	d(Ce-H) /Å
H*	0.03	0.27	0.27	2.12

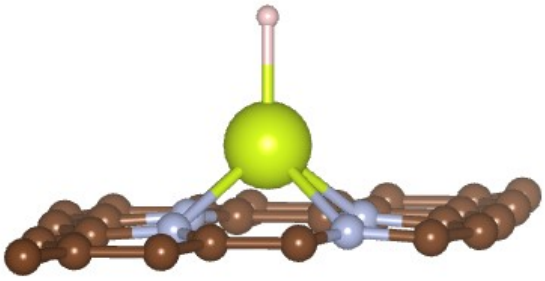

Figure S21: Adsorption configuration of H* on Ce@4N-Gr.